Published in final edited form as:
Free Radic Biol Med. 2012 January 15; 52(2): 427–435. doi:10.1016/j.freeradbiomed.2011.09.020.

Nitroglycerin drives endothelial nitric oxide synthase activation via the phosphatidylinositol 3-kinase/protein kinase B pathway

Mao Mao[a], **Varadarajan Sudhahar**[a], **Kristine Ansenberger-Fricano**[a], **Denise C. Fernandes**[b], **Leonardo Y. Tanaka**[b], **Tohru Fukai**[a], **Francisco R.M. Laurindo**[b], **Ronald P. Mason**[c], **Jeannette Vasquez-Vivar**[d], **Richard D. Minshall**[e], **Krisztian Stadler**[c], and **Marcelo G. Bonini**[a,c,*]

[a]Section of Cardiology and Department of Pharmacology, College of Medicine, University of Illinois at Chicago, Chicago, IL 60612, USA

[b]Vascular Biology Laboratory, Heart Institute (InCor), University of Sao Paulo School of Medicine, Sao Paulo, Brazil

[c]Laboratory of Pharmacology and Chemistry, National Institute of Environmental Health Sciences, National Institutes of Health, Research Triangle Park, NC 27709, USA

[d]Department of Biophysics, Medical College of Wisconsin, Milwaukee, WI 53226, USA

[e]Departments of Pharmacology and Anesthesiology, University of Illinois at Chicago, IL, 60612 USA

Abstract

Nitroglycerin (GTN) has been clinically used to treat angina pectoris and acute heart episodes for over 100 years. The effects of GTN have long been recognized and active research has contributed to the unraveling of numerous metabolic routes capable of converting GTN to the potent vasoactive messenger nitric oxide. Recently, the mechanism by which minute doses of GTN elicit robust pharmacological responses was revisited and eNOS activation was implicated as an important route mediating vasodilation induced by low GTN doses (1–50 nM). Here, we demonstrate that at such concentrations the pharmacologic effects of nitroglycerin are largely dependent on the phosphatidylinositol 3-kinase, Akt/PKB, and phosphatase and tensin homolog deleted on chromosome 10 (PTEN) signal transduction axis. Furthermore, we demonstrate that nitroglycerin-dependent accumulation of 3,4,5-$InsP_3$, probably because of inhibition of PTEN, is important for eNOS activation, conferring a mechanistic basis for GTN pharmacological action at pharmacologically relevant doses.

Keywords

Nitroglycerin; Glyceryl trinitrate; PI3K; Akt; eNOS; Nitric oxide; Free radicals

Nitroglycerin (GTN) is a powerful vasodilator that has been assumed to exert its pharmacologic effects by generating nitric oxide. The beneficial activity of GTN as a vasodilator IS well known and the mechanisms of nitroglycerin reduction to nitric oxide have been investigated for over 100 years [1]. Currently, much of the pharmacologic effects and metabolism of nitroglycerin are well documented but the mechanism by which the drug

*Corresponding author at: Section of Cardiology and Department of Pharmacology, College of Medicine, University of Illinois at Chicago, Chicago, IL 60612, USA. mbonini@uic.edu (M.G. Bonini).

elicits its effects as a vasodilator remains controversial [2–12]. Several studies have established multiple metabolic pathways through which enzymatic reduction of GTN produces nitric oxide or nitric oxide precursors [6,7,13–17]. These enzymes include xanthine oxidase [6], glutathione *S*-transferase [7,18], and more recently mitochondrial aldehyde dehydrogenase (ALDH-2) [4,16,17]. Indeed, the concerted action of ALDH-2 with the mitochondrial electron transport chain has been receiving increasing attention as a key route mediating the intramitochondrial conversion of GTN into nitrite (NO_2^-) , which could, in principle, be further reduced in mitochondria to nitric oxide by mechanisms that remain equally debatable [19,20]. Interestingly, a fairly recent study has reported that ALDH-2 knockout leads to inhibition of low-dose nitroglycerin-induced vasodilation in mice, but cellular and mechanistic effects other than a direct inhibitory action of GTN upon ALDH-2 have not been considered [2]. For instance, it is possible that aldehyde accumulation in mitochondria and oxidative stress may affect mitochondrial function and the regulation of nitric oxide synthase activity, indirectly causing endothelial irresponsiveness to nitrovasodilators/GTN. Of note, strategies have been developed to pharmacologically spare, restore, or compensate enzyme-driven GTN metabolism, which were proven to be efficient in reversing nitrate tolerance in vitro [21,22] but surprisingly have been of limited use in the clinical setting.

Alternatively, studies performed by our group demonstrated that endothelial NO synthase (eNOS) is critically involved in the amplification of the vasodilator effects elicited by low-dose GTN [3]. For example, we demonstrated that GTN induces eNOS phosphorylation in mice and rat aorta shortly after GTN treatment and that the inhibition of nitric oxide synthases is effective in preventing low-dose nitroglycerin-induced vasodilation and decreases in rat blood pressure. Our study is in agreement with previous reports that showed that GTN exposure in cultured endothelial cells leads to the accumulation of citrulline, indicative of nitric oxide synthase activation [8]. It also concurs with other studies that demonstrated that the rapid action of GTN is coincident with its peak concentrations in the plasma rather than with its lower nitrate metabolites [23,24]. Further support to the idea that eNOS intermediates nitroglycerin-induced vasodilation is found in early reports showing the endothelium dependence of GTN effects in animals and human patients [9,10,12]. In addition, it has been demonstrated that L-arginine, a nitric oxide synthase substrate, is capable of amplifying and sustaining nitroglycerin-induced nitric oxide production [25]. Although compelling, the validity of these early observations was diminished by the fact that endothelial nitric oxide synthase-knockout animals are fully responsive to GTN, a fact that remained to be reconciled with a fundamental role for the enzyme in mediating nitroglycerin-induced vasodilation [26,27]. In our work referenced in [3] we reported that neuronal (n) NOS compensates for the knocking out of eNOS and that it responds to GTN, in agreement with previous studies that showed that nNOS is overexpressed in the aortic tissue of eNOS-knockout animals, where it compensates for eNOS impairment [28]. Thus, the demonstrations that nNOS responds to GTN and that it is overexpressed in eNOS-knockout animals [28] leave little room for any doubt about an essential role for constitutive nitric oxide synthases in nitroglycerin-mediated vasodilation. One important aspect that required further investigation is the mechanism that links GTN to eNOS phosphorylation.

Here, we show, through multiple lines of evidence, that phosphatidylinositol 3-kinase (PI3K) is involved in nitroglycerin-induced vasodilation and demonstrate that activation of nitric oxide synthase through the PI3K pathway leads to nitric oxide production similar to other established signal transduction-dependent eNOS activators (i.e., vascular endothelial growth factor, VEGF). Taken together with our earlier studies, these results reinforce nitric oxide synthase activation as an important route underlying low-dose nitroglycerin-induced vasodilation while demonstrating that at pharmacologic GTN concentrations nitric oxide production is almost exclusively dependent on signal transduction pathways.

Materials and methods

Chemicals

The PI3K inhibitor wortmannin was purchased from Calbiochem (Gibbstown, NJ, USA). The protein kinase B (Akt) 1/2 inhibitor (1,3-dihydro-1-(1-((4-(6-phenyl-1*H*-imidazo[4,5-g]quinoxalin-7-yl)phenyl) methyl)-4-piperidinyl)-2*H*-benzimidazol-2-one trifluoroacetate) was from Sigma (Cat. No. A6730; St. Louis, MO, USA). Nitroglycerin was from American Regent (Shirley, NY, USA). Anti-phosphorylated eNOS (Ser 1177) was from BD Life Science and was used at 1:1000 dilution; phosphorylated PTEN (Ser 380) was from Cell Signaling Technology (Beverley, MA, USA) and phosphatase and tensin homolog deleted on chromosome 10 (PTEN) and phosphorylated Akt (Ser 473) antibodies were from Abcam (Cambridge, MA, USA) and were used at 1:1000 dilution. All other reagents were of analytical grade or better.

Cell cultures

Human and bovine aortic endothelial cells (HAEC or BAEC; Allcells, Emeryville, CA, USA), human microvascular endothelial cells (HMEC), and primary mouse endothelial cells (MEC) were cultured at 37 °C, 5% CO_2 in corresponding endothelial medium with supplements including growth factors, 10% FBS, and 1% antibiotics–antimycotics (Sigma).

Western blot assays

After lysis with RIPA buffer containing protein inhibitor cocktail (Roche's complete mini) and phosphatase inhibitors (20 mM NaF, 5 mM $NaVO_3$, 1 mM $NaVO_4$, 2.5 mM glycerol phosphate, and 10 mM sodium pyrophosphate), lysates were centrifuged and the supernatant was recovered. Proteins were separated using 4–12% Bis–Tris precast gradient gels from Invitrogen and blotted onto nitrocellulose membranes. After overnight blocking with 5% fat-free milk, specific primary and secondary antibodies were incubated with the membranes at the indicated dilutions and time. Densitometry was performed using the software ImageJ from the National Institutes of Health (NIH).

Measurement of intracellular NO production by DAF-2T (triazolofluorescein)

BAEC (passage 5 or 6) were grown to full confluence in 100-mm dishes in Dulbecco's modified Eagle's medium (DMEM) supplemented with 10% FBS. Before DAF-2 treatment, cells were pretreated with DMEM containing either wortmannin (500 nM), Akt inhibitor (20 μM), or L-NIO (0.1 mM) for 2 h, then washed twice with Dulbecco's phosphate-buffered saline (DPBS), and incubated with medium containing 5 μM DAF-2DA for 30 min to allow intracellular accumulation of DAF-2. After that the cells were further treated with 10 nM GTN, vehicle control, or VEGF (20 ng/ml) for another 30 min The experiment was finished by washing the cells twice with DPBS and scraping and collecting them in centrifuge tubes. After centrifugation (3000 rpm, 5 min) and removal of supernatant, the pellets were syringe lysed in phosphate buffer, pH 7.5, containing 100 μM diethylenetriaminepentaacetic acid and 0.1% Triton X-100. Aliquots were taken for protein determination and the remaining lysate was loaded onto a Centricon and centrifuged for 1 h at 10,000 rpm at 4 °C. Authentic DAF-2 T solution was also centrifuged through Centricons to check for recovery of the product injected onto the HPLC. DAF-2 and DAFT-2 T analysis was performed on an Agilent 1100 HPLC series system. Samples (50 μl)were separated on a Synergi-Fusion (250×4.6 mm; Phenomenex) using an isocratic elution with potassium phosphate buffer (pH 7.5, 10 mM) and 5% v/v acetonitrile, at a flow rate of 1 ml/min. Fluorescence was measured at 490 nm (excitation) and 515 nm (emission).

3,4,5-Phosphatidylinositol (3,4,5-InsP_3) measurement in nitroglycerin-treated cells

PIP3 mass strip kit was from Echelon. All other reagents were from Sigma. HMEC were cultured in 75-cm^2 flasks and used at 100% confluence. Cells were washed once with PBS and then incubated with full MCDB medium containing nitroglycerin (500 nM and 5 μM) in the presence of 5% CO_2 at 37 °C. After the indicated times the medium was aspirated and ice-cold 0.5 M trichloroacetic acid (TCA) solution was added. Cells were collected and centrifuged at 1500 rpm. The pellet was then washed twice with 5% TCA/1 mM EDTA solution. Neutral lipids were extracted by MeOH:$CHCl_3$ (2:1) solvent and discarded. Acidic lipids were extracted from the pellet by $CHCl_3$:MeOH:12 M HCl (40:80:1). After phase split the organic solvent was collected into 1.5-ml centrifuge tubes and vacuum dried. The extracted lipids were stored at −20 °C and reconstituted by sonication in $CHCl_3$: MeOH:12 M HCl (1:2:0.8) in an iced bath. Five microliters of each sample was used and the PIP3 mass strip assay was carried out according to the manufacturer's protocol. The result was quantitated in ImageJ software from NIH.

PTEN immunoprecipitation

Serum-starved mouse endothelial cells were treated with the designated stimulus. After 15 min, the medium was removed. The cells were washed twice with TRIS buffered saline (TBS) and lysed in lysis buffer containing protease inhibitors. Total protein concentration was determined by BCA assay. Each immunoprecipitation was performed using 5 μg rabbit anti-PTEN antibody (Abcam) and 20 μl anti-rabbit IgG Dynabeads (Invitrogen Dynal, Oslo, Norway).

PTEN phosphatase activity assay

Dynabeads with immunoprecipitated PTEN were washed two times with TBS and one time with phosphatase reaction buffer of 100 mM Tris–HCl (pH 8.0). After removal of the supernatant, 50 μl of reaction buffer containing 200 μM water-soluble D-myophosphatidylinositol-3,4,5-triphosphate (Echelon Biosciences, Salt Lake City, UT, USA) was added to the beads. The reaction was allowed to proceed at 37 °C for 60 min. Immunoprecipitates were centrifuged and the supernatants were placed into a 96-well plate in duplicate. Biomol Green reagent (100 μl; Enzo Life Sciences, Plymouth Meeting, PA, USA) was added into each well and the plate was incubated at room temperature for 20 min. Absorbance at 620 nm was assessed using a plate reader. Phosphate concentrations were calculated using a standard curve. Results are presented as relative PTEN activity compared with control.

Transient PTEN silencing

Primary MEC were grown in DMEM/F12 medium with supplements. At 100% confluence, the cells were washed with PBS and harvested with 0.05% trypsin–EDTA. Transfection was performed through electroporation using an Amaxa Nucleofector device following the manufacturer's protocol. For each reaction, 5×10^5 cells were mixed with 100 nM small interfering RNA (siRNA) and resuspended in 100 μl Nucleofector buffer. After electroporation, the cells were plated into six-well plates and incubated (37 °C, 5% CO_2) for 24 h. Basal NO was measured as NO_2^- accumulated in fresh (unsupplemented) medium accumulated for 4 h by chemiluminescence. After the medium was sampled, the cells were lysed for Western blot analysis of PTEN. Control siRNA and PTEN siRNA were purchased from Cell Signaling Technology.

Aortic ring assay

Rats were killed by CO_2 asphyxia. The thoracic aorta was quickly dissected, cleaned of fat and connective tissue, and cut into four rings 4–5 mm in length. The rings were mounted

under 2 g of resting tension in 15-ml organ baths containing Krebs solution (115 mM NaCl, 4.7 mM KCl, 2.5 mM $CaCl_2$, 1.14 mM KH_2PO_4, 1.19 mM $MgSO_4$, 11.1 mM glucose, and 25 mM $NaHCO_3$), gassed with 95% O_2–5% CO_2, and maintained at 37 °C. Preparations were allowed to equilibrate for 60 min with periodic washing before the experiments started. Tension was measured with a force displacement transducer (Biopac Systems MP100). In some experiments, the endothelium of aortic rings was removed by gently rubbing the intimal surface; in others, care was taken to maintain the integrity of the endothelium. Nonfunctional endothelium was tested by the inability of ACh (0.1 nM to 1 μM) to induce relaxation of aortic rings precontracted with phenylephrine (0.1 μM). Nitroglycerin (0.1 nM to 1 μM) was added to the organ bath after the addition of the PI3K inhibitor wortmannin. Aortic rings with functional endothelium exhibited at least 90% relaxation under identical conditions. Values are expressed as means±SEM. Statistical comparisons were performed through two-way ANOVA, followed by the Bonferroni test, at a 0.05 significance level (using GraphPad Prism program, version 4).

Mesenteric artery dilation assay

Isometric tension of mesenteric resistance arteries was measured using wire myograph (Model 610 M; Danish Myo Technology, Denmark). Briefly, the first- or second-order branches of resistance arteries were isolated from the mouse mesenteric bed, cut into ~2-mm segments, and stored in cold Krebs physiological salt solution (PSS; 119.0 mM NaCl, 25.0 mM $NaHCO_3$, 4.6 mM KCl, 1.2 mM $MgSO_4$, 1.8 mM $CaCl_2$, 11.0 mM glucose) at pH 7.4. The vessels were mounted in between two hooks using tungsten wire (25 μm in diameter) in an organ chamber containing Krebs PSS bubbled with a gas mixture containing 5% CO_2 and 95% O_2. Basal tension was set on arteries stretched to L_{100}, where L_{100} is defined as the circumference of the relaxed artery exposed to a transmural pressure of 100 mm Hg and equilibrated for 1 h. After equilibration, the arteries were exposed to a high concentration of KCl (80 mM) and 10 μM norepinephrine for 2–3 min until reproducible maximal contractions occurred. The α-adrenergic receptor agonist phenylephrine was added to increase basal tension to 60 to 80% of maximal KCl contraction. Cumulative concentrations (0.01–10 μM) of GTN were added to the bathing solution every 5 min. At the end of the each experiment, a cumulative concentration of sodium nitroprusside (0.01–10 μM) was added to the bath to demonstrate the intact smooth muscle function. Results are expressed as percentage relaxation of the phenylephrine-treated rings, with 100% relaxation representing basal tension.

Animal studies

Male Sprague–Dawley rats weighing 150–200 g were used throughout the study. In each set of experiments, rats were anesthetized with a mixture of ketamine (100 mg/kg) and xylazine (20 mg/kg). Wortmannin and Akt 1/2 inhibitor (1,3-dihydro-1-(1-((4-(6-phenyl-1*H*-imidazo[4,5-g]quinoxalin-7-yl)phenyl)methyl)-4-piperidinyl)-2*H*-benzimidazol-2-one trifluoroacetate) were injected intraperitoneally, 2 h before nitroglycerin administration at a concentration of 0.5 (wortmannin) or 2 mg/kg (Akt inhibitor) dissolved in dimethyl sulfoxide (DMSO). Blood pressure measurements were performed by the tail-cuff method (Model SC1000; Hatteras Instruments) by using blood pressure analysis application software (version 2.21). Rats were placed on a warm pad after anesthesia, and a cuff equipped with a photon-sensor device was fitted over the tail. The cuff was set with a maximum pressure of 220 mm Hg. After 30 consecutive measurements (30 min), 4 mg of crushed NitroTab pill was given sublingually to the rats, and blood pressure was monitored for an additional 30 min. Mice used in the experiments included PI3Kp110γ-knockout animals obtained from Dr. Asrar Malik (Department of Pharmacology at UIC) and respective controls.

Chemiluminescence measurement of NO_2^- accumulation

NO_2^- was quantified by chemiluminescence using General Electric NOA 280i equipment. Briefly the medium was sampled and injected into a reacting chamber containing NaI/acetic acid (75%) under vacuum accordingly to the manufacturers' instructions.

Statistical Analysis

Statistical analysis was performed with GraphPad InStat by using one-way ANOVA with Student–Newman–Keuls comparison. For selected experiments *t* test was used as indicated in the figure legends. A value of $P<0.05$ was considered significant, whereas a value of $P<0.01$ was considered highly significant.

Results

Nitric oxide production from low-dose GTN is dependent on PI3K and eNOS

HAEC were exposed to GTN (10 nM) for 30 min in the presence of the nitric oxide probe DAF-2. Nitric oxide production was evaluated by the HPLC analysis of the product DAF-2T. In Fig. 1, results are shown demonstrating that, similar to VEGF (a signal transduction agent that elicits eNOS activity via receptor-dependent activation of PI3K/Akt/eNOS), 10 nM GTN significantly increased nitric oxide production, which could be inhibited by the PI3K inhibitor wortmannin, the Akt inhibitor (Akti 1/2 trifluoroacetate salt hydrate), and the eNOS inhibitor L-NIO. These results are consistent with our hypothesis that low-dose GTN, like VEGF, stimulates NO production via PI3K/Akt-dependent nitric oxide synthase activation. Results were confirmed by the analysis of NO_2^- (the nitric oxide autoxidation product) accumulation in the medium of HAEC treated with GTN using chemiluminescence (data not shown).

PI3K inhibition blunts GTN-induced vasodilation

Pharmacologic inhibition of PI3K with wortmannin (50 nM) and genetic knockout approaches were used to examine the involvement of PI3K in nitroglycerin-induced vasodilation in two types of vascular tissue, isolated rat aortic rings and mouse mesenteric arteries. Fig. 2A, left, confirms the inhibitory effect of wortmannin pretreatment upon acetylcholine-elicited vasorelaxation. This result is not surprising because cholinergic activation of NO production is known to be dependent on the PI3K/Akt pathway [29]. Consistent with a role for PI3K in mediating GTN-induced eNOS activation, Fig. 2A, right, shows that wortmannin was efficient in significantly reducing GTN-dependent vasodilation at the low-dose (<50 nM). In agreement with previous findings, signal transduction-dependent pathways seemed to be prevalent at low (<50 nM) but not at high GTN doses (>50 nM) [3]. Similar to wortmannin, Akt 1/2 inhibitor increased the GTN EC_{50}, showing that Akt 1/2 inhibition turns the vessels less sensitive to GTN (Fig. 2B). This result is consistent with Akt 1/2 involvement in the mediation of low-dose GTN-induced vasodilation. The results obtained with the PI3K pharmacological inhibitor wortmannin were repeated using mesenteric arteries obtained from genetic knockout mice lacking the p110γ catalytic subunit of the endothelium relevant PI3Kγ isoform. As shown in Fig. 2C, p110γ-knockout animals are resistant to nitroglycerin-induced vasodilation at low doses but not at high doses, confirming that PI3K-dependent signal transduction is a prevalent pathway leading to low-dose nitroglycerin-induced effects. Fig. 2B, right, shows that p110γ-knockout animals had normal responses to sodium nitroprusside (a direct NO-donor compound), which confirmed that these animals had functional vascular functions downstream of NO. Although the effects in the genetically depleted tissue are reduced in comparison to chemical inhibition, which suggests redundancy among the various PI3K isoforms, the fact that arterial pressure is related to the fourth power of the vessel diameter

by the Hagen–Poiseuille equation highlights the significance of p110γ-mediated signaling in GTN-dependent blood pressure reduction.

PI3K/Akt inhibition blunts GTN-induced blood pressure decreases in rats

To ascertain the pharmacological relevance of PI3K-mediated nitric oxide synthase activation in response to vasodilation, rats were subjected to blood pressure measurements after exposure to GTN. Naïve controls treated with GTN showed pronounced decreases in the diastolic blood pressure momentarily after sublingual administration according to previous observations [3] (Fig. 3). Similar to nitric oxide inhibitors [3], the pretreatment of the animals with the PI3K inhibitor wortmannin led to a marked inhibition of the nitroglycerin-induced decrease in the blood pressure. This result confirms that pharmacological dose nitroglycerin-induced vasodilation is mediated through signal transduction events downstream of PI3K. Inhibition of Akt 1/2 had a similar effect, confirming the participation of endothelium-prevalent Akt 1 and possibly Akt 2 in GTN-dependent vasodilation, presumably through eNOS function.

PI3K inhibition decreases nitroglycerin-induced eNOS activation in endothelial cells

In Fig. 4, we sought to demonstrate that GTN-induced eNOS activation is mediated by the PI3K/Akt pathway. Phosphorylation of eNOS at the activation site Ser 1179 was assessed in BAEC after treatment with 500 nM GTN. Indeed, marked eNOS activation was observed momentarily (3 min) after the exposure of cells to GTN added to the medium, according to previous observations [3]. Pretreatment of the cells with wortmannin, a PI3K inhibitor, strongly inhibited the phosphorylation of eNOS, indicating that PI3K is an upstream effector of GTN-induced eNOS activation. Consistently, inhibition of Akt led to a pronounced diminishment of GTN-dependent eNOS phosphorylation similar to that obtained in the case of wortmannin. Taken together with Fig. 1, these results are in agreement with the PI3K/Akt pathway being fundamentally involved in low-dose nitroglycerin-induced eNOS-dependent nitric oxide production by endothelial cells. The results obtained with BAEC were recapitulated in HMEC (Fig. 6B). In addition, we sought to determine whether GTN had an effect on the regulation of the enzyme PTEN, which is an important regulator of the PI3K/Akt axis. Indeed, it has been claimed that the chemical basis of GTN-induced ALDH-2 inhibition is the relatively rapid reaction of the ALDH-2 low pK_a active thiolate moiety with the nitrate ester groups of GTN, producing a thiol nitrate that decays, producing NO_2^- and the oxidized inactive enzyme. Similarly, PTEN, which is localized predominantly in the cytosol and in the vicinity of the plasma membrane (the port of entry of GTN into the cell), is a low pK_a thiol phosphatase, thus likely to be reactive toward GTN. In cells, PTEN normally opposes PI3K activity by degrading the PI3K product, 3,4,5-InsP_3. Through its lipid phosphatase activity PTEN reduces 3,4,5-InsP_3 levels, deactivating Akt. Fig. 6B shows Akt activation simultaneous to PTEN inhibition elicited by 500 nM GTN instantaneously after its addition to the cell culture medium. Fig. 5A, shows the concentration-dependent activation of Akt (as evaluated from the phosphorylation of its activation site Ser 473) by GTN. Importantly, Akt phosphorylation occurred rapidly after GTN addition to BAEC and HMEC cultures (Figs. 4, 5, and 6),which paralleled the sustained activation of eNOS and PTEN inhibition (evaluated through the phosphorylation of its inhibitory site Ser 380, Fig. 6) [29]. Notably, the time courses of PTEN inhibition and Akt and eNOS activation closely matched those of GTN-induced decreases in blood pressure in animals ([3], this work Fig. 3). Net increases in 3,4,5-InsP_3 (the product of PI3K activity and the substrate of PTEN) were also assessed to confirm GTN-induced PTEN inhibition in HMEC at 2 and 5 min. Consistent with Akt activation and PTEN inhibition (Fig. 6B), 3,4,5-InsP_3 levels were significantly increased at 2 min and reached fivefold higher levels at 5 min post GTN (Fig. 7A). To further demonstrate that PTEN inhibition is sufficient to elicit endogenous nitric oxide production we transiently silenced PTEN using siRNA (Fig. 7D). Consistent with

previously published studies that demonstrated that PTEN silencing results in increased Akt and eNOS phosphorylation, our experiments demonstrated that PTEN knockdown elicits nitric oxide production independent of GTN, thus consubstantiating our proposal that GTN-driven PTEN inhibition leads to nitric oxide production by promoting unchecked PI3K signaling.

PTEN inhibition by GTN treatment raises cellular 3,4,5-InsP_3 level

Our experiments shown in Figs. 6 and 7A–C indicated that PTEN activity is diminished by GTN. Thus, we aimed at directly measuring PTEN activity post-GTN treatment in endothelial cells. We immunopurified PTEN from cell lysates and assessed its activity by measuring the rates of dephosphorylation of 3,4,5-D-myo-inositol triphosphate, a water-soluble PTEN substrate. HMEC were then treated with GTN (0.5 and 5 μM) and were lysed 5 min after GTN addition. As shown in Fig. 7C, PTEN was significantly inhibited by GTN at the lowest tested concentration. This observation is in full agreement with our proposal that by inhibiting PTEN, GTN activates eNOS via the PI3K/Akt pathway.

Discussion

Certainly, much of the pharmacology and metabolism of GTN have been unraveled over 100 years of intense investigation. Nevertheless, fundamental questions have existed pertaining to the molecular mechanisms that link the administration of minute doses of GTN in the clinic to the robust and momentary pharmacologic effects such doses elicit in patients. Various studies have indicated that eNOS is activated by GTN in endothelial cells and that eNOS substrates/cofactors contribute to maximize the effects of GTN as a vasodilator and attenuate GTN resistance [8,11,25]. These studies have supported a role for eNOS activation in mediating the drug-induced vasodilation. In contrast, another set of investigations has argued against a fundamental role for eNOS in mediating GTN-induced pharmacologic and toxic effects upon the vasculature. These studies have claimed that metabolic routes sustain NO production from GTN and that their inactivation is causative of GTN tolerance [2,17]. Although we believe that metabolic routes contribute to GTN-induced effects, particularly at higher doses, our recent observations are consistent with the first set of studies that found endogenous NO production as the cause of nitroglycerin-mediated vasodilation.

Indeed, we recently presented directed evidence demonstrating that eNOS phosphorylation occurs momentarily after GTN administration [3] and that NO recovery from GTN-treated cells is comparable to that elicited by classical activators of signal transduction such as VEGF (this work, Fig. 1). Likewise, L-NIO, an irreversible inhibitor of constitutive nitric oxide synthases significantly reduced NO production from endothelial cells exposed to GTN and VEGF ([3], and Fig. 1). Notably, the similar inhibitory effects were attained through the use of PI3K and Akt inhibitors, which are known upstream activators of agonist elicited NO production by eNOS. The relevance of the PI3K/Akt pathway for GTN-induced vasodilation was further demonstrated in Fig. 2 through the pharmacologic inhibition of each enzyme and validated in mesenteric arteries of genetic knockout animals. Importantly, Fig. 2 demonstrates that in either case (inhibitor studies or genetic knockout) significant attenuation of GTN effects is achieved at pharmacologically relevant doses of GTN (<50 nM) but not at higher concentrations, at which metabolic conversion of GTN to NO is likely to prevail. The studies presented in Fig. 2 are in close agreement with previously published results that demonstrated the efficacy of NO inhibitors or endothelial removal in preventing low-dose (<50 nM) but not high-dose nitroglycerin-induced vasodilation [3]. Not surprisingly, pronounced effects of GTN in diminishing diastolic blood pressure in rats were markedly reduced when the animals were pretreated with wortmannin or Akt inhibitor (Fig. 3). Taken together, these results constitute compelling evidence implicating signal transduction pathways in the mediation of GTN's pharmacological effects by activating

eNOS. Indeed, studies performed with endothelial cells and presented in Fig. 4 demonstrated that 0.5 μM GTN instantaneously induced the phosphorylation of eNOS at the activation site Ser 1177, which was fully inhibited by either PI3K or Akt inhibitor. These studies were recapitulated in human endothelial microvascular cells (Fig. 6). In both BAEC and HMEC, eNOS phosphorylation was temporally paralleled by Akt activation, indicating the involvement of the PI3K/Akt pathway in GTN-induced eNOS activation. Interestingly, we also found that PTEN, the enzyme that opposes PI3K activity by degrading 3,4,5-$InsP_3$, was rapidly inhibited by GTN. PTEN inhibition was determined through the Western blot analysis of the inhibitory site Ser 380 phosphorylation and through the quantification of the active second messenger 3,4,5-$InsP_3$ (Figs. 7A and B). PTEN inhibition was further confirmed by the measurement of PTEN activity after immunopurification from lysates of cells previously exposed to GTN (Fig. 7C). Therefore, we propose that GTN rapidly inactivates PTEN in endothelial cells leading to the accumulation of 3,4,5-$InsP_3$. Higher 3,4,5-$InsP_3$ levels arising from the unopposed PI3K activity lead to Akt and eNOS activation (schematically represented in Fig. 8). Importantly, PTEN lipid phosphatase activity is dependent on the critical active residue Cys 124. In its reduced form the low-pK_a Cys 124 thiolate catalyzes the removal of the 3-phosphate group of 3,4,5-phosphatidylinositol in remarkable similarity to the proposed and widely accepted mechanism of ALDH-2 inhibition by GTN. However, different from ALDH-2, which is confined in mitochondria, PTEN, which is itself fairly sensitive to inhibition by oxidants and by electrophiles, resides predominantly in the cytosol, specifically at the vicinity of the plasma membrane, and is thus more likely to interact with diffusible xenobiotics upon their entry into the cell. Indeed, the fundamental role of ALDH-2 in GTN bioconversion to NO was claimed largely on the basis of knockout studies that showed that ALDH-2-knockout animals are less responsive to low-dose GTN than ALDH-2-competent animals. Nevertheless, depletion of ALDH-2 has been linked to increased oxidative stress and vascular dysfunction [30–32] probably because of increased levels of reactive species (aldehydes and oxidants) production. Hence, with the currently available data it is impossible to distinguish whether the GTN-tolerant phenotype exhibited by the ALDH-2-knockout animal is a consequence of its inability to convert GTN to NO or, alternatively, is attributable to dysregulation of oxidant-sensitive signal transduction pathways such as the PI3K/Akt/PTEN axis.

Aldehydes and oxidants can potentially lead to persistent inactivation of PTEN [33] and eNOS aberrant activation, which is claimed to be a cause of vascular dysfunction in several publications [34–37]. eNOS and, secondary to it, endothelial dysfunction may be a consequence of ALDH-2 deficiency, explaining the unresponsive phenotype of the ALDH-2-knockout animals independent of ALDH-2 enzymatic activity. Consistent with this possibility, recent studies have demonstrated that ALDH-2 depletion causes vascular dysfunction, seemingly because of a higher superoxide radical anion production by mitochondria, which further reduces NO availability while producing the strong oxidant peroxynitrite [33,38]. Therefore, a definitive role for ALDH's intermediacy in low-dose GTN-induced vasodilation is pending the verification that in ALDH-2-knockouts increased $O_2^{\bullet -}$, oxidative stress, and aldehyde accumulation do not critically affect GTN-mediated signaling or consume NO, thus limiting its biological actions. In a recent study, we directly demonstrated that GTN is capable of inducing eNOS phosphorylation at the activation site Ser 1177 in the aorta of animals and that nitric oxide inhibition is sufficient to attenuate both the decrease in blood pressure and the response of isolated aortic rings to low-dose GTN [3]. In addition, we showed that at low doses (<50 nM) GTN-induced vasodilation is dependent on the endothelium and correlates temporally with eNOS activation in accordance with previously published work [9,12]. These results, the earlier studies showing eNOS activation by GTN in cells, and the demonstrated dependence of PI3K on the GTN-induced eNOS activation reported here leave little space for any doubt about the involvement of nitric oxide

synthases and signal transduction pathways in low-dose GTN-induced effects. At high concentrations (>50 nM) metabolism-driven routes are likely to be dominant, as previously shown by us and others [2,3,39,40] and confirmed here by the demonstration that at high GTN doses inhibition of PI3K/Akt does not result in attenuation of GTN-induced vasodilation (Fig. 2). Because metabolic processes are dependent on enzymatic reactions governed by rate laws, it is expected that such pathways would be favored by high but not low doses, in which case amplification of a signal by an array of interdependent and highly efficient transducers should prevail.

In summary, we have demonstrated that by inhibiting PTEN, GTN augments Akt and eNOS activities, which mediate the low-dose effects of GTN on the vasculature (please see schematic representation in Fig. 8). The mechanisms underlying the activity of GTN as a powerful vasodilator are determined by dose and depend on multiple intricate mechanisms, which involve signal transduction and metabolic bioactivation. The demonstration that GTN, like other electrophiles, is capable of inducing PI3K/Akt/eNOS activation through PTEN inhibition may serve as a cornerstone warranting further studies focused on the cellular adaptations that trigger GTN tolerance and nitroglycerin-induced vascular dysfunction by affecting cellular signaling networks.

Acknowledgments

The authors are indebted to Drs. Asrar Malik and Xiaopei Gao for the generous gifts of PI3Kp110γ-knockout mice and mouse endothelial cells. We thank Dr. Ann Motten for the careful review of the manuscript. These studies were supported in part by the National Institute of Environmental Health Sciences Division of Intramural Research, an American Heart Association Scientist Development grant (09SDG2250933 to M.G.B.), and a National Heart Lung and Blood grant (R01 HL070187 to T.F.). The authors also thank the Fundacao de Amparo a Pesquisa do Estado de Sao Paulo and Conselho Nacional de Pesquisa de Desenvolvimento Cientifico e Tecnologico for financial support to F.R.M.L.

References

1. Bond GS. Effect of various agents on the blood flow through the coronary arteries and veins. J. Exp. Med. 1910; 12:575–585. [PubMed: 19867344]
2. Chen Z, Foster MW, Zhang J, Mao L, Rockman HA, et al. An essential role for mitochondrial aldehyde dehydrogenase in nitroglycerin bioactivation. Proc. Natl. Acad. Sci. U. S. A. 2005; 102:12159–12164. [PubMed: 16103363]
3. Bonini MG, Stadler K, Silva SO, Corbett J, Dore M, et al. Constitutive nitric oxide synthase activation is a significant route for nitroglycerin-mediated vasodilation. Proc. Natl. Acad. Sci. U. S. A. 2008; 105:8569–8574. [PubMed: 18562300]
4. Sydow K, Daiber A, Oelze M, Chen Z, August M, et al. Central role of mitochondrial aldehyde dehydrogenase and reactive oxygen species in nitroglycerin tolerance and cross-tolerance. J. Clin. Invest. 2004; 113:482–489. [PubMed: 14755345]
5. Kleschyov AL, Oelze M, Daiber A, Huang Y, Mollnau H, et al. Does nitric oxide mediate the vasodilator activity of nitroglycerin? Circ. Res. 2003; 93:e104–e112. [PubMed: 14551241]
6. Millar TM, Stevens CR, Benjamin N, Eisenthal R, Harrison R, et al. Xanthine oxidoreductase catalyses the reduction of nitrates and nitrite to nitric oxide under hypoxic conditions. FEBS Lett. 1998; 427:225–228. [PubMed: 9607316]
7. Hill KE, Hunt RW Jr, Jones R, Hoover RL, Burk RF. Metabolism of nitroglycerin by smooth muscle cells: involvement of glutathione and glutathione S-transferase. Biochem. Pharmacol. 1992; 43:561–566. [PubMed: 1540213]
8. Abou-Mohamed G, Kaesemeyer WH, Caldwell RB, Caldwell RW. Role of L-arginine in the vascular actions and development of tolerance to nitroglycerin. Br. J. Pharmacol. 2000; 130:211–218. [PubMed: 10807657]

9. Schwarz M, Katz SD, Demopoulos L, Hirsch H, Yuen JL, et al. Enhancement of endothelium-dependent vasodilation by low-dose nitroglycerin in patients with congestive heart failure. Circulation. 1994; 89:1609–1614. [PubMed: 8149528]
10. Forster C, Main JS, Armstrong PW. Endothelium modulation of the effects of nitroglycerin on blood vessels from dogs with pacing-induced heart failure. Br. J. Pharmacol. 1990; 101:109–114. [PubMed: 2126476]
11. Gruhn N, Aldershvile J, Boesgaard S. Tetrahydrobiopterin improves endothelium-dependent vasodilation in nitroglycerin-tolerant rats. Eur. J. Pharmacol. 2001; 416:245–249. [PubMed: 11290375]
12. Gruhn N, Boesgaard S, Andersen C, Aldershvile J. Nitroglycerin tolerance: different mechanisms in vascular segments with or without intact endothelial function. J. Cardiovasc. Pharmacol. 2002; 40:201–209. [PubMed: 12131549]
13. Kenkare SR, Han C, Benet LZ. Correlation of the response to nitroglycerin in rabbit aorta with the activity of the Mu class glutathione S-transferase. Biochem. Pharmacol. 1994; 48:2231–2235. [PubMed: 7811305]
14. Zhang J, Chen Z, Cobb FR, Stamler JS. Role of mitochondrial aldehyde dehydrogenase in nitroglycerin-induced vasodilation of coronary and systemic vessels: an intact canine model. Circulation. 2004; 110:750–755. [PubMed: 15289380]
15. Zhang XJ, Chang L, Zhang YM, Deng S, Li YJ, et al. Comparing the role of glutathione-S-transferase and mitochondrial aldehyde dehydrogenase in nitroglycerin biotransformation and the correlation with calcitonin gene-related peptide. Eur. J. Pharmacol. 2009; 617:97–101. [PubMed: 19576883]
16. Chen Z, Stamler JS. Bioactivation of nitroglycerin by the mitochondrial aldehyde dehydrogenase. Trends Cardiovasc. Med. 2006; 16:259–265. [PubMed: 17055381]
17. Daiber A, Wenzel P, Oelze M, Schuhmacher S, Jansen T, et al. Mitochondrial aldehyde dehydrogenase (ALDH-2)—maker of and marker for nitrate tolerance in response to nitroglycerin treatment. Chem. Biol. Interact. 2009; 178:40–47. [PubMed: 18834868]
18. Matsuzaki T, Sakanashi M, Nakasone J, Noguchi K, Miyagi K, et al. Effects of glutathione S-transferase inhibitors on nitroglycerin action in pig isolated coronary arteries. Clin. Exp. Pharmacol. Physiol. 2002; 29:1091–1095. [PubMed: 12390297]
19. Munzel T, Daiber A, Mulsch A. Explaining the phenomenon of nitrate tolerance. Circ. Res. 2005; 97:618–628. [PubMed: 16195486]
20. Kollau A, Beretta M, Russwurm M, Koesling D, Keung WM, et al. Mitochondrial nitrite reduction coupled to soluble guanylate cyclase activation: lack of evidence for a role in the bioactivation of nitroglycerin. Nitric Oxide. 2009; 20:53–60. [PubMed: 18951990]
21. Beretta M, Sottler A, Schmidt K, Mayer B, Gorren AC. Partially irreversible inactivation of mitochondrial aldehyde dehydrogenase by nitroglycerin. J. Biol. Chem. 2008; 283:30735–30744. [PubMed: 18786921]
22. Wenzel P, Hink U, Oelze M, Schuppan S, Schaeuble K, et al. Role of reduced lipoic acid in the redox regulation of mitochondrial aldehyde dehydrogenase (ALDH-2) activity: implications for mitochondrial oxidative stress and nitrate tolerance. J. Biol. Chem. 2007; 282:792–799. [PubMed: 17102135]
23. Culling W, Singh H, Bashir A, Griffiths BE, Dalal JJ, et al. Haemodynamics and plasma concentrations following sublingual GTN and intravenous, or inhaled, isosorbide dinitrate. Br. J. Clin. Pharmacol. 1984; 17:125–131. [PubMed: 6422972]
24. Yu DK, Williams RL, Benet LZ, Lin ET, Giesing DH. Pharmacokinetics of nitroglycerin and metabolites in humans following oral dosing. Biopharm. Drug Dispos. 1988; 9:557–565. [PubMed: 3147725]
25. Parker JO, Parker JD, Caldwell RW, Farrell B, Kaesemeyer WH. The effect of supplemental L-arginine on tolerance development during continuous transdermal nitroglycerin therapy. J. Am. Coll. Cardiol. 2002; 39:1199–1203. [PubMed: 11923046]
26. Otto A, Fontaine J, Berkenboom G. Ramipril treatment protects against nitrate-induced oxidative stress in eNOS−/− mice: an implication of the NADPH oxidase pathway. J. Cardiovasc. Pharmacol. 2006; 48:842–849. [PubMed: 16891913]

27. Otto A, Fontaine J, Tschirhart E, Fontaine D, Berkenboom G. Rosuvastatin treatment protects against nitrate-induced oxidative stress in eNOS knockout mice: implication of the NAD(P)H oxidase pathway. Br. J. Pharmacol. 2006; 148:544–552. [PubMed: 16633368]
28. Talukder MA, Fujiki T, Morikawa K, Motoishi M, Kubota H, et al. Up-regulated neuronal nitric oxide synthase compensates coronary flow response to bradykinin in endothelial nitric oxide synthase-deficient mice. J. Cardiovasc. Pharmacol. 2004; 44:437–445. [PubMed: 15454851]
29. Miller SJ, Lou DY, Seldin DC, Lane WS, Neel BG. Direct identification of PTEN phosphorylation sites. FEBS Lett. 2002; 528:145–153. [PubMed: 12297295]
30. Wenzel P, Schuhmacher S, Kienhofer J, Muller J, Hortmann M, et al. Manganese superoxide dismutase and aldehyde dehydrogenase deficiency increase mitochondrial oxidative stress and aggravate age-dependent vascular dysfunction. Cardiovasc. Res. 2008; 80:280–289. [PubMed: 18596060]
31. Shearn CT, Smathers RL, Stewart BJ, Fritz KS, Galligan JJ, et al. Phosphatase and tensin homolog deleted on chromosome 10 (PTEN) inhibition by 4-hydroxynonenal leads to increased Akt activation in hepatocytes. Mol. Pharmacol. 2011; 79:941–952. [PubMed: 21415306]
32. Delgado-Esteban M, Martin-Zanca D, Andres-Martin L, Almeida A, Bolanos JP. Inhibition of PTEN by peroxynitrite activates the phosphoinositide-3-kinase/Akt neuroprotective signaling pathway. J. Neurochem. 2007; 102:194–205. [PubMed: 17302912]
33. Connor KM, Subbaram S, Regan KJ, Nelson KK, Mazurkiewicz JE, et al. Mitochondrial H_2O_2 regulates the angiogenic phenotype via PTEN oxidation. J. Biol. Chem. 2005; 280:16916–16924. [PubMed: 15701646]
34. Pannirselvam M, Verma S, Anderson TJ, Triggle CR. Cellular basis of endothelial dysfunction in small mesenteric arteries from spontaneously diabetic (db/db−/−) mice: role of decreased tetrahydrobiopterin bioavailability. Br. J. Pharmacol. 2002; 136:255–263. [PubMed: 12010774]
35. Leopold JA, Loscalzo J. Organic nitrate tolerance and endothelial dysfunction: role of folate therapy. Minerva Cardioangiol. 2003; 51:349–359. [PubMed: 12900717]
36. Zou MH, Cohen R, Ullrich V. Peroxynitrite and vascular endothelial dysfunction in diabetes mellitus. Endothelium. 2004; 11:89–97. [PubMed: 15370068]
37. Zhao YY, Zhao YD, Mirza MK, Huang JH, Potula HH, et al. Persistent eNOS activation secondary to caveolin-1 deficiency induces pulmonary hypertension in mice and humans through PKG nitration. J. Clin. Invest. 2009; 119:2009–2018. [PubMed: 19487814]
38. Daiber A, Oelze M, Wenzel P, Wickramanayake JM, Schuhmacher S, et al. Nitrate tolerance as a model of vascular dysfunction: roles for mitochondrial aldehyde dehydrogenase and mitochondrial oxidative stress. Pharmacol. Rep. 2009; 61:33–48. [PubMed: 19307691]
39. Yuan R, Sumi M, Benet LZ. Investigation of aortic CYP3A bioactivation of nitroglycerin in vivo. J. Pharmacol. Exp. Ther. 1997; 281:1499–1505. [PubMed: 9190888]
40. Beretta M, Gruber K, Kollau A, Russwurm M, Koesling D, et al. Bioactivation of nitroglycerin by purified mitochondrial and cytosolic aldehyde dehydrogenases. J. Biol. Chem. 2008; 283:17873–17880. [PubMed: 18450747]

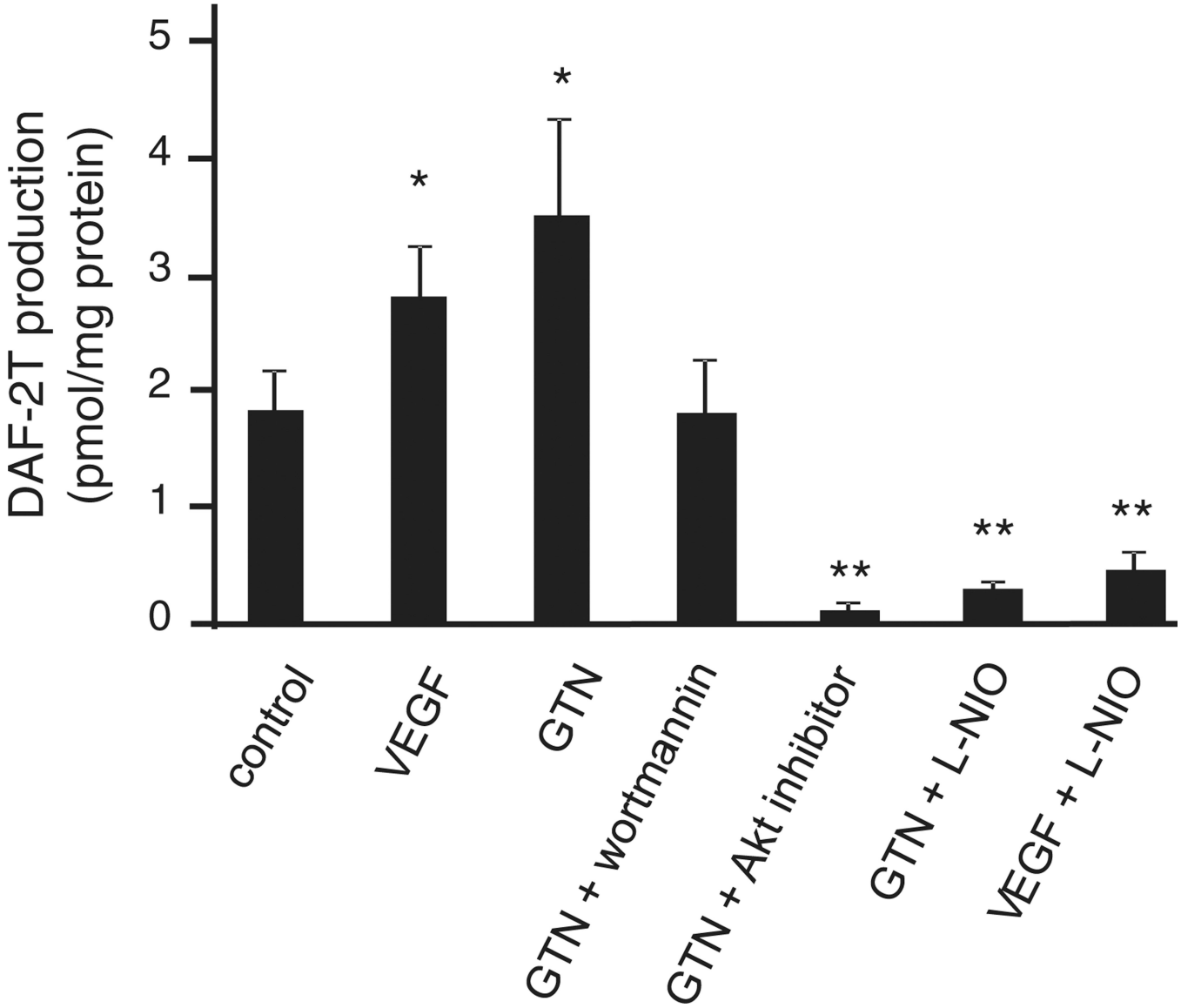

Fig. 1.

Intracellular NO measurement by HPLC analysis of DAF-2 T (triazolofluorescein). HAEC were pretreated with wortmannin (500 nM), Akt inhibitor (20 μM), or L-NIO (0.1 mM) before addition of DAF-2 (5 μM) and tandem treatments with GTN (10 nM) or VEGF (20 ng/ml). Cellular concentrations of the product DAF-2 T were analyzed by HPLC and calculated using a standard curve. Reported data are DAF-2 T concentration normalized to protein content in each sample. **P*<0.05, ***P*<0.01.

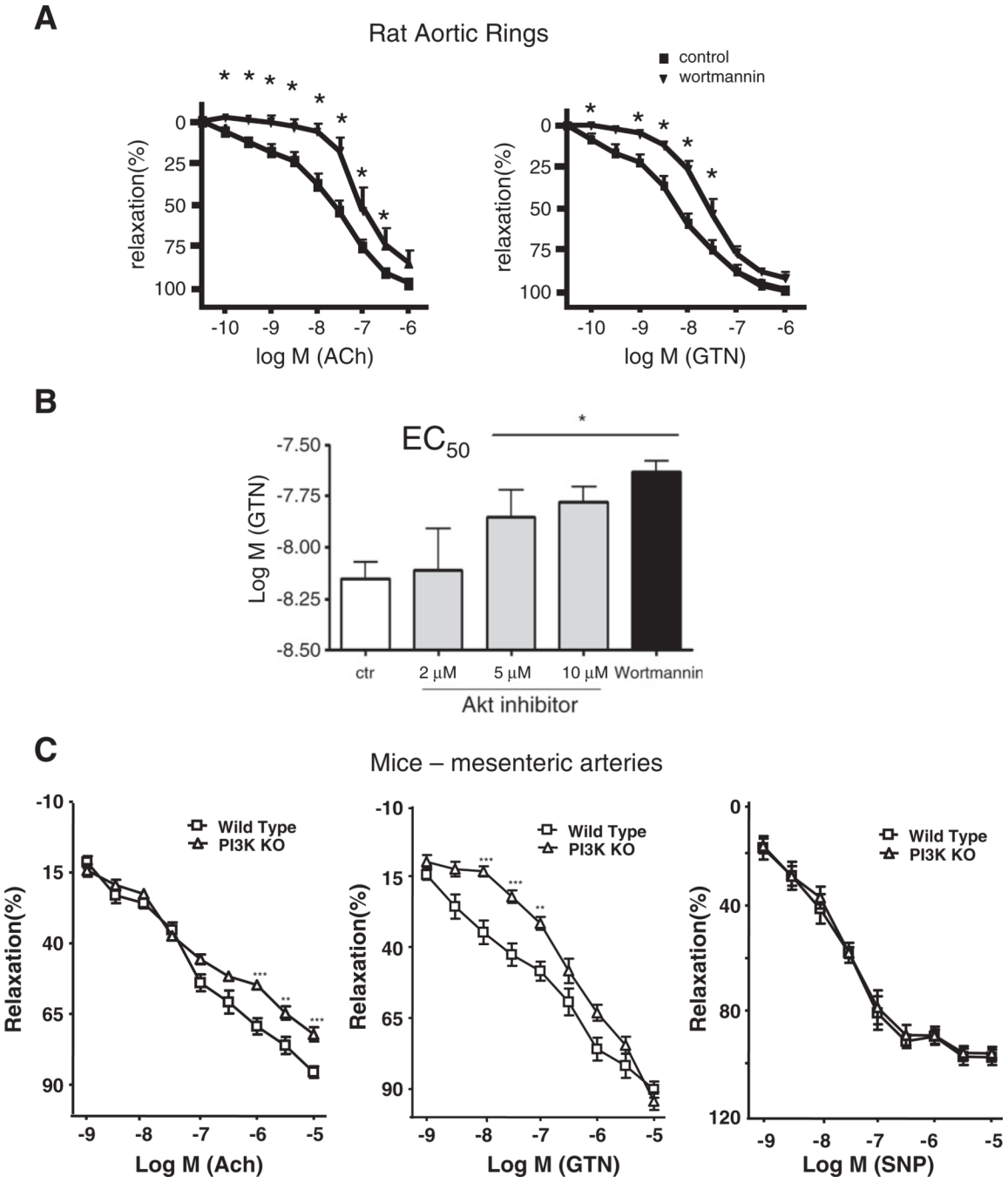

Fig. 2.

PI3K involvement in GTN-dependent vasodilation. (A) Effect of wortmannin (PI3K inhibitor) pretreatment upon the acetylcholine (Ach)- or GTN-induced dilation of rat aortic rings. (B) Nitroglycerin EC_{50} values measured in rat aortic rings in the presence of the indicated concentrations of Akt 1/2 inhibitor. (C) Vasodilation experiment with mesenteric tissue recovered from p110γ-knockout mice. p110γ is the catalytic subunit of endothelial PI3K enzyme. Both pharmacologic inhibition and genetic knockout of PI3K inhibited GTN-induced dilation of conducing (aorta) and resistant (mesenteric artery) vessels. *P<0.05, **P<0.01.

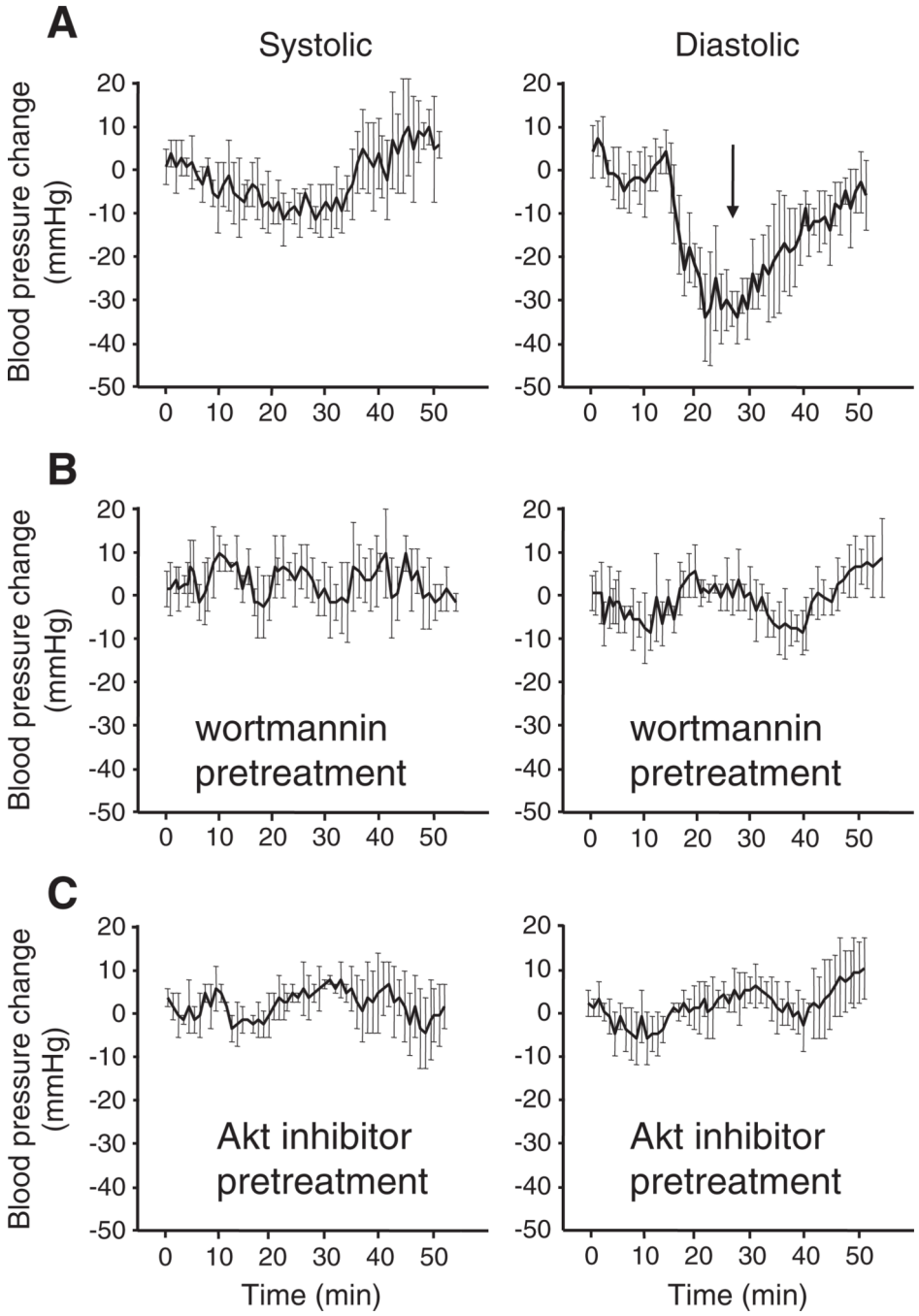

Fig. 3.

Assessment of PI3K and Akt inhibition effects upon GTN-induced blood pressure decreases in anesthetized rats. Experiments were performed using the tail-cuff method. Animals were anesthetized with ketamine/xylazine mixtures according to the Materials and methods. Blood pressure was stabilized for at least 20 min before GTN administration. Wortmannin (0.5 mg/kg) or Akt inhibitor (2 mg/kg) was administrated 2 h before the experiments in DMSO (50 μL injection volume). Controls received DMSO injection equivalent to the amount required for inhibitor treatment 2 h before GTN.

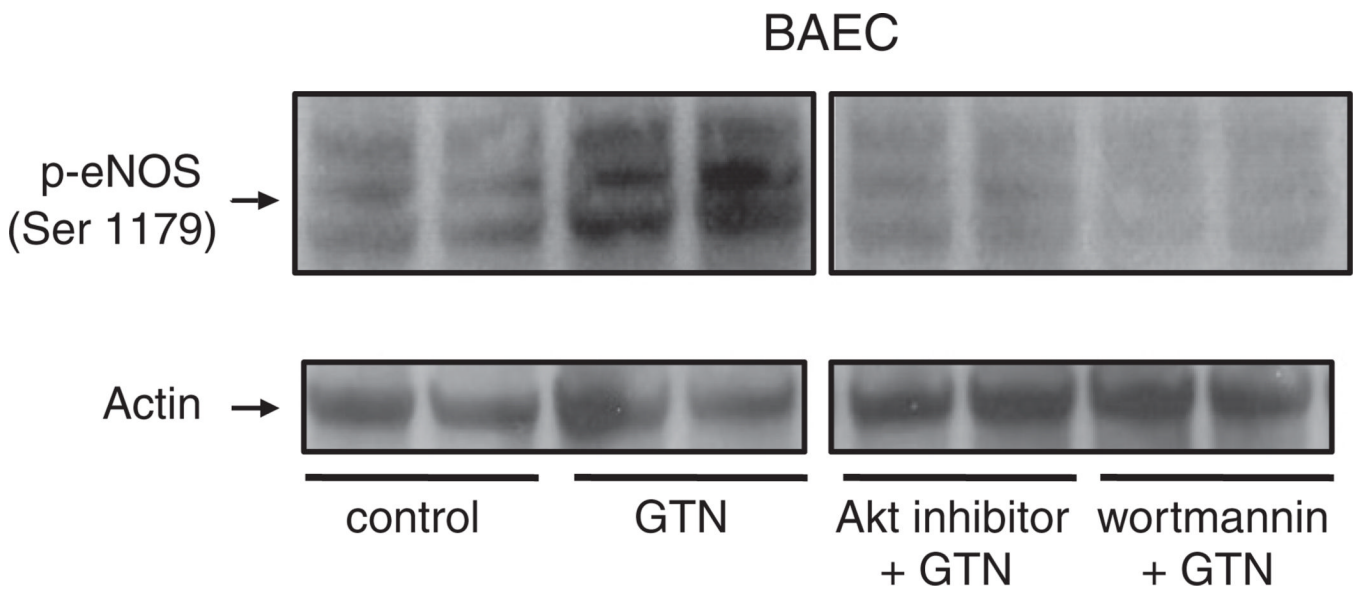

Fig. 4.

PI3K/Akt-dependent phosphorylation of eNOS elicited by nitroglycerin. BAEC were challenged with nitroglycerin (500 nM) for 3 min before harvest. PI3K inhibitor wortmannin (100 nM) or Akt inhibitor (20 μM) was dissolved in DMSO and added to the cell cultures 1 h before GTN treatment; DMSO was also added at the same concentration (v/v) to control groups. Final DMSO concentration did not exceed 0.1%.

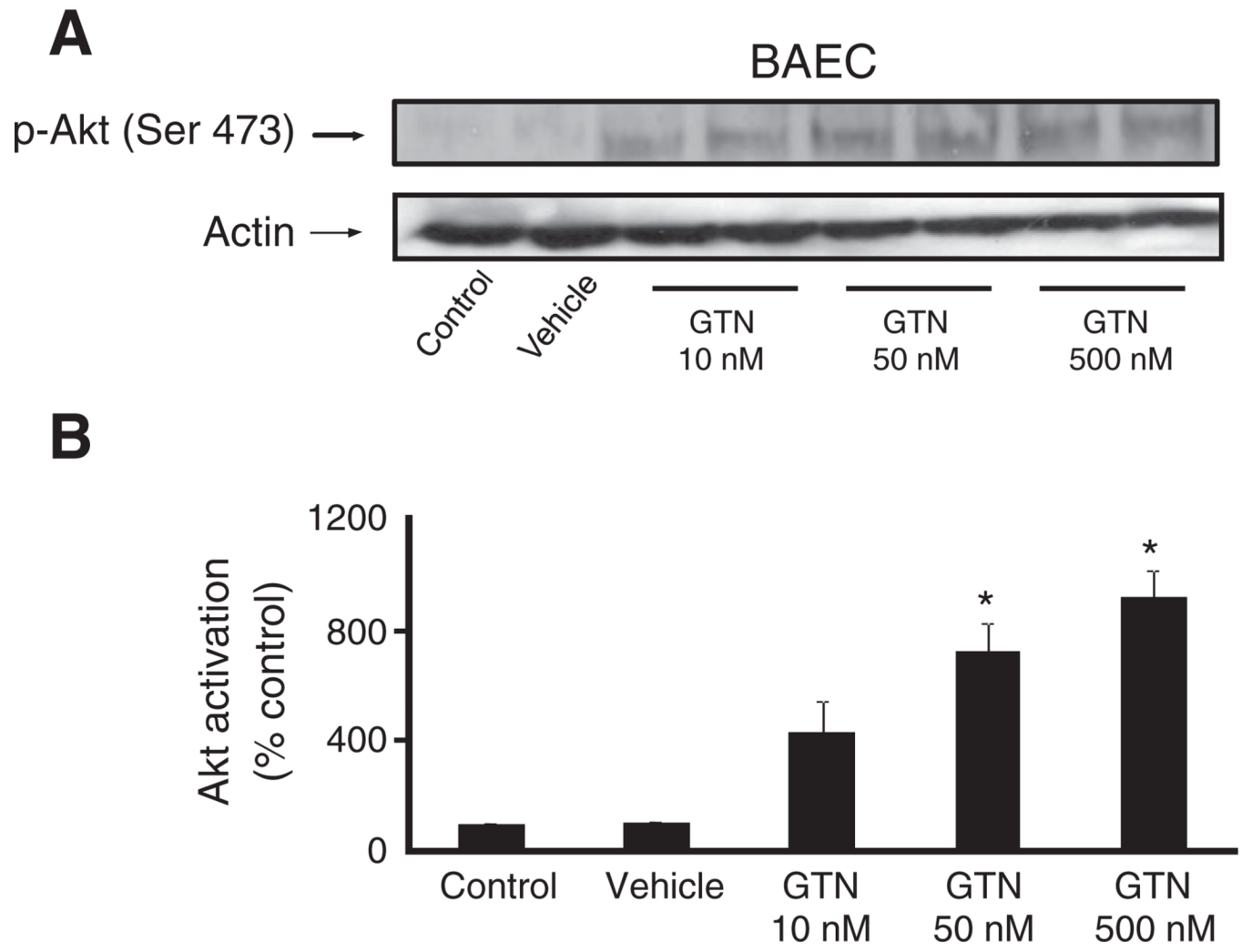

Fig. 5.

Concentration-dependent Akt activation by GTN. (A) BAEC cells were treated with vehicle control (30% ethanol, 30% propylene glycol, 40% water) or the indicated GTN concentrations for 3 min before harvest. (B) Band densities were measured using ImageJ software. Results were quantified as relative Akt activation compared with control; **P*<0.05 by Student's *t* test.

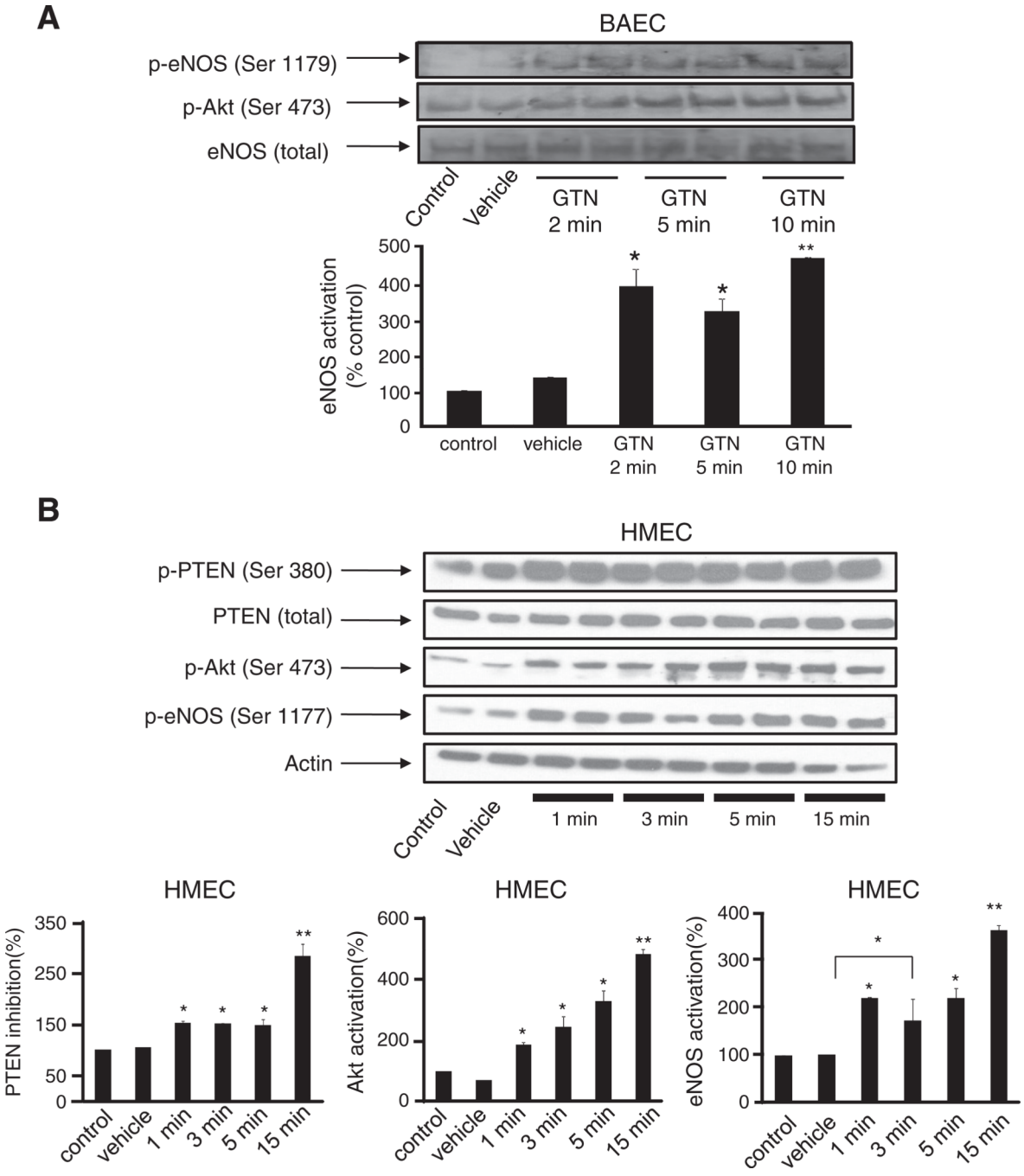

Fig. 6.

Time-dependent activation of Akt and eNOS paralleling PTEN phosphorylation by GTN. Representative Western blots showing PTEN phosphorylation (Ser 380), eNOS phosphorylation (Ser 1177 or 1179), and Akt phosphorylation (Ser 473) in (A) BAEC and (B) HMEC treated with vehicle or 500 nM GTN for the indicated amounts of time. Vehicle was added for 10 min in (A) and 15 min in (B). Results show rapid and sustained eNOS phosphorylation at the activation site Ser 1177, Akt phosphorylation at the activation site Ser 473, and PTEN phosphorylation at the inhibitory site Ser 380 by 500 nM GTN. Band intensities for phosphorylated eNOS in BAEC and for the experiments performed with

HMEC were quantified using ImageJ and the values are reported as density units relative to control; *P<0.05, **P<0.01.

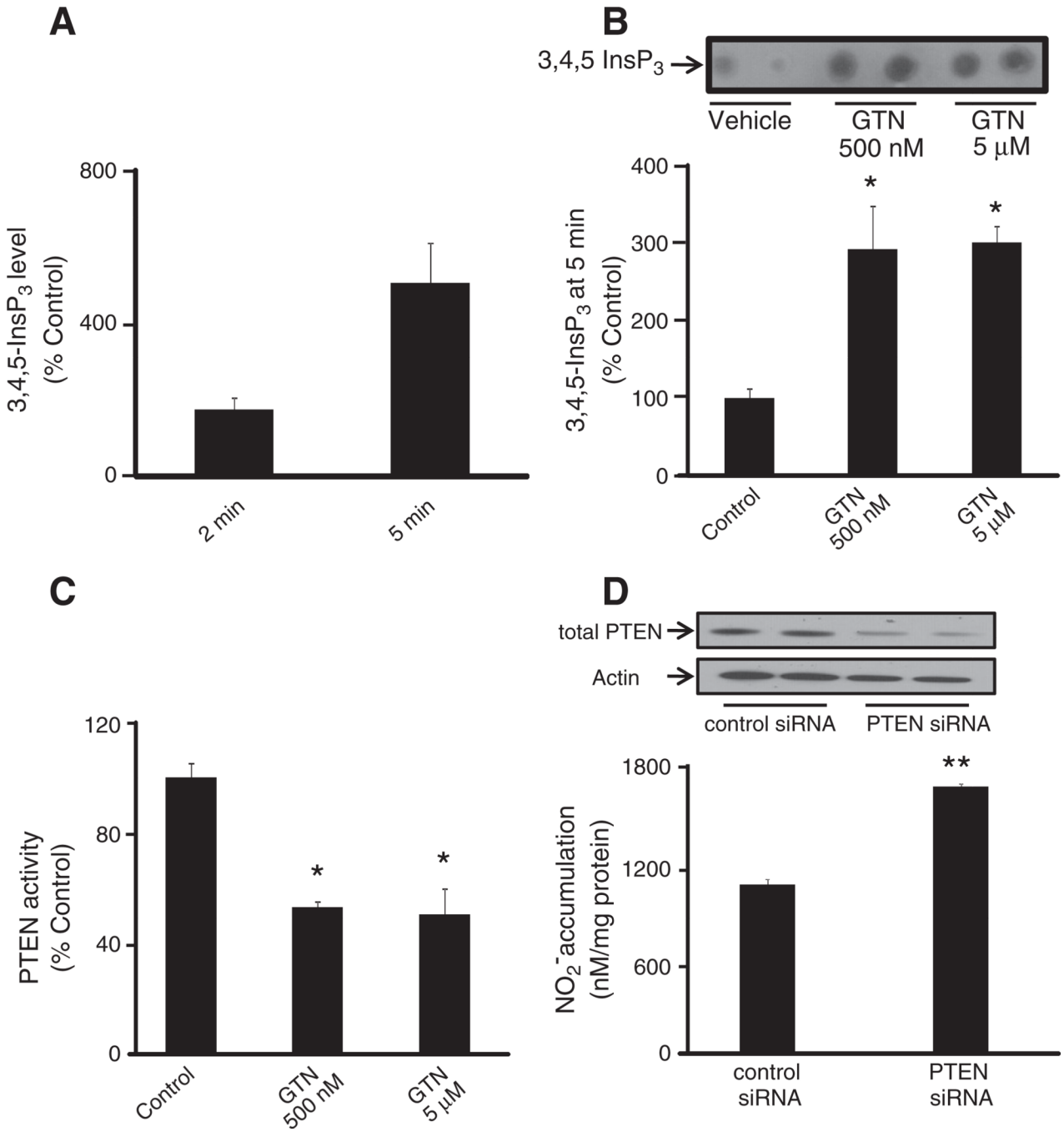

Fig. 7.

GTN treatment elaborates cellular 3,4,5-$InsP_3$ level by inhibiting PTEN activity. (A) Measurement of 3,4,5-$InsP_3$ level as a time-dependent response to GTN treatment. HMEC were treated with 500 nM GTN for 2 and 5 min. Results are shown relative to control. (B) Mass strip blot of PTEN substrate 3,4,5-$InsP_3$ in HMEC treated with vehicle or GTN for 15 min. Results are shown relative to control. (C) Measurement of immunoprecipitated PTEN phosphatase activity by Biomol green assay. Three independent experiments were performed and the results reveal PTEN inhibition consistent with increase in 3,4,5-$InsP_3$ levels. The values are reported as phosphate release relative to control; *P<0.05 by Student's t test. (D) PTEN silencing by siRNA in MEC and subsequent measurement of basal NO

production was assessed by the chemiluminescence-based quantification of NO_2^- accumulation in medium. Results show mean values of four independent measurements; $^{**}P<0.01$. Quantification of band densities was performed using Image software.

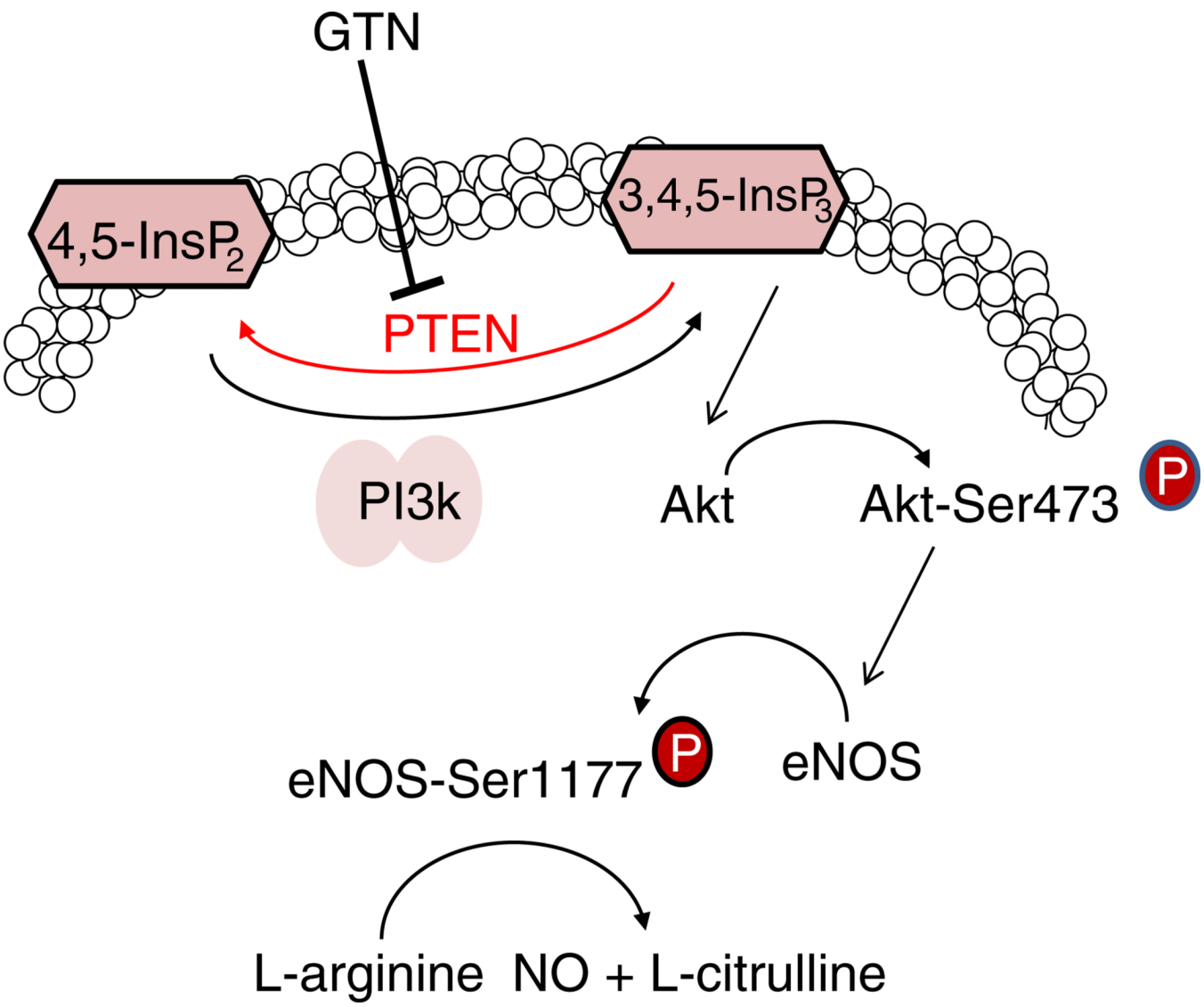

Fig. 8.
Representation of the proposed mechanism of GTN-induced eNOS activation via PTEN inhibition.